ELSEVIER

Journal of Photochemistry and Photobiology A: Chemistry 103 (1997) 257–264

Journal of PHOTOCHEMISTRY AND PHOTOBIOLOGY A: CHEMISTRY

Heterogeneous photocatalysis XV. Mechanistic aspects of cadmium sulfide-catalyzed photoaddition of olefins to Schiff bases

Wolfram Schindler, Horst Kisch *

Institut für Anorganische Chemie der Universität Erlangen-Nürnberg, Egerlandstraße 1, D-91058, Erlangen, Germany

Received 26 September 1996; accepted 6 November 1996

Abstract

A methanolic suspension of cadmium sulfide powder photocatalyzes the addition of cyclopentene and cyclohexene to imines affording γ,δ-unsaturated amines and the hydrodimer of the imine as a by-product. The product ratio is not dependent on the light intensity, but changes in favor of the hydrodimer when the amount of photocatalyst is increased. Measurement of the imine dark adsorption reveals the presence of multilayer adsorption. At concentrations below 0.5 mmol l^{-1}, Langmuir behavior is observed, from which an adsorption equilibrium constant of 4400 ± 950 l mol^{-1} can be calculated for the imine; the value obtained by a novel "in situ" determination of the dependence of the initial rate on the imine concentration affords a value of 2000 l mol^{-1}. The adsorption constants of cyclopentene and cyclohexene, as determined from the conventional rate–concentration dependence, are in the region of 15 l mol^{-1} and suggest that both olefins adsorb onto the same surface sites. This is supported by competition experiments. © 1997 Elsevier Science S.A.

Keywords: Adsorption; Cadmium sulfide; Photocatalysis; Semiconductor; γ,δ-Unsaturated amines

1. Introduction

The mechanisms of photoreactions catalyzed by semiconductor powder suspensions can be understood in terms of the single crystal model developed for photoelectrochemical cells [1,2]. In this, charge separation is produced within the inhomogeneous electric field of a space charge layer formed at the solid–liquid interface. For small particles of very low charge carrier density, as present in most slurry-type experiments, the depth of this layer should exceed the particle diameter due to the very low charge carrier density, and charge separation is brought about by the competition between recombination and interfacial electron transfer to and from the substrates [3]. Since the lifetime of the electron–hole pair is usually in the region of nanoseconds [4], only substrates adsorbed onto the semiconductor surface can successfully compete with recombination. Therefore a reaction may be photocatalyzed only when, in addition to a match between the substrate redox potential and the semiconductor band position (which is often not known exactly for the powders employed), favorable substrate adsorption is possible [5,6]. In this context, it is noted that the substrate adsorption may also change the photophysical properties of the solid–liquid interface itself, i.e. the efficiency of charge separation, and therefore straightforward interpretations of adsorptive effects may lead to wrong conclusions [5,7,8].

Hitherto reported semiconductor-catalyzed reactions fall into two categories. In type A reactions, which correspond to conventional photoelectrolysis, two or more products are formed. Type B reactions lead to only one single product and can be considered as "paired photoelectrolysis" (a rare example is known from electrolysis at microelectrodes [9]). In the latter case, the primary redox intermediates combine to give one unique end-product. While many type A reactions are known, only a few type B transformations have been reported. To the latter belong the CdS-catalyzed photoaddition of cyclic olefins to 1,2-diazenes [10] or imines [11] reported recently from our laboratory. A simplified mechanism of the imine reaction (Scheme 1) is summarized in Eqs. (1)–(9) (see below) [11].

Illumination of the CdS powder affords electron–hole pairs which are trapped at reactive (e_r^-, h_r^+) or unreactive (e_{ur}^-, h_{ur}^+) surface sites (Eqs. (1)–(3)) (for simplicity, the equation describing the formation of the unreactive electron–hole pair is omitted in Eqs. (1)–(9)). In competition with elec-

* Corresponding author. Tel.: +49 9131 857361; fax: +49 9131 857363; e-mail: kisch@anorganik.chemie.uni-erlangen.de

PII S1010-6030(96)04556-X

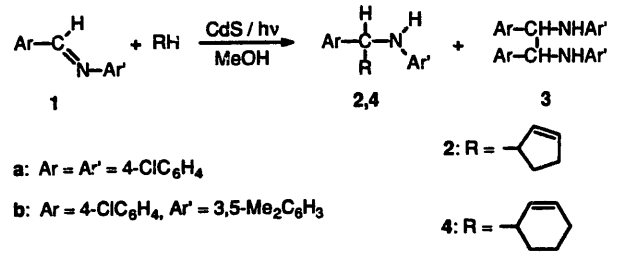

a: Ar = Ar' = 4-ClC$_6$H$_4$

b: Ar = 4-ClC$_6$H$_4$, Ar' = 3,5-Me$_2$C$_6$H$_3$

Scheme 1.

tron–hole pair recombination, proton-coupled electron transfer to the adsorbed imine **1** affords the corresponding α-aminobenzyl radical (Eq. (5)) and oxidation and deprotonation of adsorbed cyclopentene (R–H) lead to an allyl radical (Eq. (6)). Although it is not known at which surface sites the interfacial electron transfer steps (Eq. (5) and Eq. (6)) occur, on the basis of the present knowledge of the chemical nature of the electron–hole pair [12], it seems probable that reduction occurs at cadmium and oxidation at sulfur sites. Heterocoupling of the two radicals finally affords the addition products **2** (Eq. (7), Scheme 1). Thus the two primary products of the redox steps are combined to give one single product and the overall process can therefore be described as "paired photoelectrolysis". In a competitive reaction, the α-aminobenzyl radicals undergo homocoupling producing the hydrodimers **3** (Eq. (8)). The corresponding dehydrodimers of R–H (Eq. (9)) can be isolated in the case of 1-phenylcyclohexene [11]. It should be noted that the formation of **2** is a $1e^-/1h^+$ process, whereas the formation of **3** requires $2e^-/2h^+$.

$$CdS \xrightarrow{h\nu} CdS(h^+/e^-) \quad (1)$$

$$CdS(h^+/e^-) \xrightarrow{k_{fc}} CdS + \Delta T + h\nu' \quad (2)$$

$$CdS(h^+/e^-) \xrightarrow{k_{tr}} CdS(h_r^+/e_r^-) \quad (3)$$

$$h_r^+ + e_r^- \xrightarrow{k_{rc}} \Delta T + h\nu'' \quad (4)$$

$$ArCH{=}NAr'_{ad} + e_r^- + H_{ad}^+ \xrightarrow{k_{red}} Ar\dot{C}H{-}NHAr'_{ad} \quad (5)$$

$$R{-}H_{ad} + h_r^+ \xrightarrow{k_{ox}} \dot{R}_{ad} + H_{ad}^+ \quad (6)$$

$$Ar\dot{C}H{-}NHAr' + \dot{R} \xrightarrow{k_{add}} ArRCH{-}NHAr' \quad (7)$$

$$2Ar\dot{C}H{-}NHAr \xrightarrow{k_{dim}} \begin{matrix} ArCH{-}NHAr' \\ | \\ ArCH{-}NHAr' \end{matrix} \quad (8)$$

$$2\dot{R} \xrightarrow{k_{dim}} R_2 \quad (9)$$

However, some basic questions, e.g. whether the C–C coupling reaction steps (Eq. (7) and Eq. (8)) proceed between adsorbed or fully solvated radicals and which factors control the product ratio, remain unanswered. We therefore investigated the influence of the light intensity and photocatalyst concentration on the rate and product ratio, and also measured the extent of substrate adsorption by different methods. In the literature, experimental evidence for adsorbed intermediates has usually been obtained by measuring the reaction rate as a function of the substrate concentration (for a summary, see Refs. [7,8]). From the linear plot of the reciprocal rate vs. the reciprocal concentration, a pseudo-adsorption constant can be calculated. Only in a few cases has the true equilibrium constant been measured in conventional adsorption experiments [7,8,13]. For the well-investigated TiO_2-catalyzed photo-oxidation of alcohols and phenols, it has been shown that the adsorption constant may be much higher or lower than the pseudo-constant, depending on the solvent employed [7].

2. Experimental details

2.1. General methods

Methanol was dried over $Mg(OCH_3)_2$, distilled and stored under N_2; the Schiff bases **1a** and **1b** were synthesized according to the literature from the corresponding benzaldehyde and aniline; cyclopentene and cyclohexene were distilled and stored under N_2. Nuclear magnetic resonance (NMR) spectroscopy was performed using a Jeol FT-JNM-EX 270 instrument (tetramethylsilane (TMS) as internal standard). IR spectroscopy was carried out using a Perkin–Elmer 983. Mass spectrometry (MS) was performed with a Varian Mat 212 (70 eV). For cyclic voltammetry, a potentiostat (PAR 264 A), glassy carbon working electrode (Rotel A), Ag/AgCl reference electrode and Pt counter-electrode were used; the solvent was CH_3CN at a substrate concentration of 10^{-3} mol l^{-1}; tetrabutylammonium hexafluorophosphate was used as electrolyte, the internal standard was ferrocene and a scan rate of 50 mV s^{-1} was employed. All concentration measurements were performed by high performance liquid chromatography (HPLC) (Knauer HPLC pump 64; semi-preparative pump head with 20 μl sample loop; column, Spherisorb ODS2 (250 mm × 8 mm, 5 μm, Knauer) with pre-column (30 mm × 8 mm); eluent, CH_3CN–H_2O (5 : 1, v/v); flow rate, 5.0 ml min^{-1}; detection, Knauer UV–visible filter-photometer at $\lambda = 254$ nm). Irradiations were performed in a cylindrical 15 ml quartz cuvette on an optical train equipped with an Osram XBO 150 W xenon arc lamp; this was installed in a light condensing lamp housing (PTI, A 1010 S); a cut-off filter of $\lambda > 400$ nm (Schott glass) was used; $I_0(\lambda = 400\text{–}520\ nm) = 2.0 \times 10^{-6}$ einstein s^{-1} cm^{-2} or 1.1×10^{-5} einstein s^{-1} cm^{-2} refer to the 5.7 cm^2 irradiated area of the quartz cuvette, estimated from iron oxalate actinometry data at 280–345 nm.

2.2. Preparation and characterization of CdS

A solution of 24.0 g (0.1 mol) of $Na_2S \cdot 9H_2O$ in 200 ml of H_2O and a solution of 25.7 g (0.1 mol) of $CdSO_4 \cdot 8/3H_2O$

in 200 ml of H_2O were added dropwise and simultaneously to 200 ml of H_2O. Stirring was continued for 12 h and the powder was washed by multiple decanting with H_2O. After separation by suction filtration, the residue was dried over P_2O_5 in a desiccator. The ground powder was heated at 150 °C and reduced pressure for 5 h (gravimetric weight loss, 4%–8%), thoroughly ground again in an agate mortar to an orange powder and stored under N_2. Microanalysis CdS (144.47): found: S, 21.62%; C, 0.13%; H, 0.15%; N, 0.00%; calculated: S, 22.19%; particle size, 1–50 μm; specific surface area, 60–80 $m^2 g^{-1}$ (BET, N_2).

2.3. Determination of the equilibrium adsorption constant

From a methanolic solution containing **1a** at different concentrations, c_0 was determined as the average value of four measurements. To 5.0 ml of this solution, 50.0 mg (0.35 mmol) of CdS was added. The suspension was sonicated for 15 min and stirred at ambient temperature (20±3 °C) overnight. From each sample, CdS was filtered off through micropore filters (more than 0.2 μm) and an average value of c_{eq} was determined as described above. The amount of adsorbed **1a** per gram of CdS (n_{eq}) was calculated from the concentration difference $c = c_0 - c_{eq}$ by dividing by a factor of ten (referring to the 10 g l^{-1} of CdS used).

2.4. Rate dependence on the imine concentration

To 50.0 mg (0.35 mmol) of CdS and 21.0 ml of a methanolic solution containing **1a** at concentrations of 2.50, 1.30, 0.54 and 0.30 mmol l^{-1} was added 11.4 mmol of cyclopentene. The mixture was sonicated for 15 min under N_2, since the reaction is very sensitive to traces of oxygen. Irradiations were performed in a 15 ml quartz cuvette. Small aliquots were taken from the suspension, CdS was filtered off through a micropore filter and the concentration of **1a** was measured. The following reaction rates were calculated from the slopes of imine concentration vs. time plots (conventional method): (a) 2.50 mmol l^{-1}, rate = 1.27×10^{-7} mol l^{-1} s^{-1}; (b) 1.30 mmol l^{-1}, rate = 0.55×10^{-7} mol l^{-1} s^{-1}; (c) 0.54 mmol l^{-1}, rate = 0.30×10^{-7} mol l^{-1} s^{-1}; (d) 0.30 mmol l^{-1}, rate = 0.23×10^{-7} mol l^{-1} s^{-1}; pseudo-adsorption constant according to Eq. (13), $K_r = 530\pm60$ l mol^{-1}.

From the concentration vs. time curves of the above experiments, the different rates were obtained as described for the "in situ" method in the text. From these, the adsorption constants K_i were calculated according to Eq. (13) (slope m' and intercept b' of the double-reciprocal plot): (a) 2.50 mmol l^{-1}, $m' = (1.61\pm0.13)\times10^4$ s, $b' = (3.14\pm0.80)\times10^7$ l s mol^{-1}, correlation coefficient 0.99, $K_i = 1960\pm430$ l mol^{-1}; (b) 1.30 mmol l^{-1}, $m' = (4.07\pm0.31)\times10^4$ s, $b' = (7.05\pm1.71)\times10^7$ l s mol^{-1}, correlation coefficient 0.99, $K_i = 1740\pm360$ l mol^{-1}; (c) 0.54 mmol l^{-1}, $m' = (7.41\pm1.20)\times10^4$ s, $b' = (13.61\pm5.41)\times10^7$ l s mol^{-1}, correlation coefficient 0.95, $K_i = 1940\pm660$ l mol^{-1}; (d) 0.30 mmol l^{-1}, $m' = (6.80\pm0.34)\times10^4$ s, $b' = (16.45\pm5.73)\times10^7$ l s mol^{-1}, correlation coefficient 0.99, $K_i = 2420\pm700$ l mol^{-1}.

The experiment was repeated with the same reaction conditions as above, but sonicated for 3 h. Values of the rate(calcd) were calculated according to Eq. (13) using $K = 4400$ l mol^{-1} and $k'_{red} = 4.0\times10^{-7}$ mol l^{-1} s^{-1} taken from the intercept of the double-reciprocal plot in Fig. 4: (a) 0.19 mmol l^{-1}, rate(exp) = 0.35×10^{-7} mol l^{-1} s^{-1}, rate(calcd) = 2.4×10^{-7} mol l^{-1} s^{-1}; (b) 0.30 mmol l^{-1}, rate(exp) = 0.56×10^{-7} mol l^{-1} s^{-1}, rate(calcd) = 2.8×10^{-7} mol l^{-1} s^{-1}; (c) 0.71 mmol l^{-1}, rate(exp) = 0.93×10^{-7} mol l^{-1} s^{-1}, rate(calcd) = 3.2×10^{-7} mol l^{-1} s^{-1}; (d) 1.60 mmol l^{-1}, rate(exp) = 2.03×10^{-7} mol l^{-1} s^{-1}, rate(calcd) = 3.5×10^{-7} mol l^{-1} s^{-1}; (e) 3.20 mmol l^{-1}, rate(exp) = 2.15×10^{-7} mol l^{-1} s^{-1}, rate(calcd) = 3.6×10^{-7} mol l^{-1} s^{-1}; (f) 8.50 mmol l^{-1}, rate(exp) = 3.6×10^{-7} mol l^{-1} s^{-1}, rate(calcd) = 3.7×10^{-7} mol l^{-1} s^{-1}; pseudo-adsorption constant according to Eq. (13), $K_r = 520\pm90$ mol l^{-1}.

2.5. Rate dependence on the cyclopentene/cyclohexene concentration

2.5.1. Cyclopentene

CdS (15.0 mg, 0.10 mmol) and 15.0 ml of a methanolic solution containing 7.0 mmol l^{-1} of **1a** and different concentrations of cyclopentene were suspended by sonication for 15 min under N_2. Irradiation was performed as described above. The reaction rates were measured from the initial slope of the imine concentration vs. time plot. From these values, the rate of imine disappearance (0.20×10^{-7} mol l^{-1} s^{-1}) in the absence of olefin, due to the oxidation of MeOH and the formation of hydrodimers [11], was subtracted from the rate at different olefin concentrations: $c_0 = 0.04$ mol l^{-1}, rate = 1.3×10^{-7} mol l^{-1} s^{-1}; $c_0 = 0.075$ mol l^{-1}, rate = 2.4×10^{-7} mol l^{-1} s^{-1}; $c_0 = 0.10$ mol l^{-1}, rate = 2.6×10^{-7} mol l^{-1} s^{-1}; $c_0 = 0.19$ mol l^{-1}, rate = 2.9×10^{-7} mol l^{-1} s^{-1}; $c_0 = 0.38$ mol l^{-1}, rate = 3.0×10^{-7} mol l^{-1} s^{-1}; $c_0 = 0.60$ mol l^{-1}, rate = 3.2×10^{-7} mol l^{-1} s^{-1}; $c_0 = 0.75$ mol l^{-1}, rate = 3.3×10^{-7} mol l^{-1} s^{-1}.

2.5.2. Cyclohexene

CdS (50.0 mg, 0.28 mmol) and 15.0 ml of a methanolic solution containing 3.0 mmol l^{-1} of **1a** and different concentrations of cyclohexene were suspended by sonication for 15 min under N_2. Irradiation and rate determination were performed as described above: $c_0 = 0.025$ mol l^{-1}, rate = 0.4×10^{-7} mol l^{-1} s^{-1}; $c_0 = 0.05$ mol l^{-1}, rate = 0.75×10^{-7} mol l^{-1} s^{-1}; $c_0 = 0.25$ mol l^{-1}, rate = 1.3×10^{-7} mol l^{-1} s^{-1}; $c_0 = 0.49$ mol l^{-1}, rate = 1.4×10^{-7} mol l^{-1} s^{-1}; $c_0 = 0.99$ mol l^{-1}, rate = 1.5×10^{-7} mol l^{-1} s^{-1}.

2.6. Rate dependence on the light intensity

CdS (50.0 mg, 0.35 mmol), **1a** (25.0 mg, 0.10 mmol), cyclopentene (0.5 ml, 5.7 mmol), MeOH (14.0 ml) and H_2O

(0.5 ml) were irradiated as described above. The light intensity was varied by neutral grey filters (Schott glass) NG4 and NG11 (50% and 32% transmission). Each value was determined three times and the average value is reported. H_2O as proton source [11] was added to enhance the reaction. $I_{rel}=17\%$, rate $=(1.2\pm0.3)\times10^{-7}$ mol l^{-1} s^{-1}; $I_{rel}=32\%$, rate $=(2.5\pm0.4)\times10^{-7}$ mol l^{-1} s^{-1}; $I_{rel}=50\%$, rate $=(3.75\pm0.15)\times10^{-7}$ mol l^{-1} s^{-1}; $I_{rel}=100\%$, rate $=(5.0\pm0.25)\times10^{-7}$ mol l^{-1} s^{-1}.

2.7. Rate and product ratio dependence on the amount of CdS

Compound **1a** (25.0 mg, 0.10 mmol), cyclopentene (0.5 ml, 5.7 mmol), MeOH (14.0 ml) and H_2O (0.5 ml) were irradiated as described above in the presence of variable amounts (0–100 mg, 0–0.7 mmol) of CdS.

2.8. Competitive reaction of cyclopentene and cyclohexene with 1b

Compound **1b** (100.0 mg, 0.40 mmol), CdS (50 mg, 0.35 mmol) and 20.0 ml of a methanolic solution containing 20.0 mmol of cyclopentene and/or cyclohexene were irradiated as described above.

Cyclopentene: rate (**1b**), 1.80×10^{-7} mol l^{-1} s^{-1}; rate (**2b**), 0.55×10^{-7} mol l^{-1} s^{-1}; rate (**3b**), 0.63×10^{-7} mol l^{-1} s^{-1}. Cyclohexene: rate (**1b**), 0.55×10^{-7} mol l^{-1} s^{-1}; rate (**3b**), 0.08×10^{-7} mol l^{-1} s^{-1}; rate (**4b**), 0.38×10^{-7} mol l^{-1} s^{-1}. Cyclopentene, cyclohexene: rate (**1b**), 1.15×10^{-7} mol l^{-1} s^{-1}; rate (**2b**), 0.25×10^{-7} mol l^{-1} s^{-1}; rate (**3b**), 0.32×10^{-7} mol l^{-1} s^{-1}; rate (**4b**), 0.18×10^{-7} mol l^{-1} s^{-1}.

3. Results and discussion

3.1. Dark adsorption of 1a

The adsorption of **1a** onto CdS was measured in methanolic solution at concentrations in the range $c_0=10^{-3}$–10^{-5} mol l^{-1}. The differences between the initial (c_0) and equilibrium (c_{eq}) concentrations were in the region of 5%–10% of c_0. A plot of the number of moles of **1a** adsorbed per gram of CdS as a function of c_{eq} is depicted in Fig. 1.

At low concentrations ($c_{eq}<0.5$ mmol l^{-1}), the data resemble a Langmuir-type adsorption isotherm, from which the maximum surface concentration $(n_{eq})_{max}$ of 20×10^{-7} mol g^{-1} can be estimated, as indicated by the broken line in the figure. At higher concentrations, a linear correlation seems to be present. The overall dependence suggests a multilayer adsorption of **1a** [14,15]. A similar behavior was also observed for the adsorption of chlorophenols onto TiO_2 [8].

The experimental determination of the adsorption equilibrium constant for concentrations below 0.5 mmol l^{-1} was performed according to the method of Hiemenz [14] which

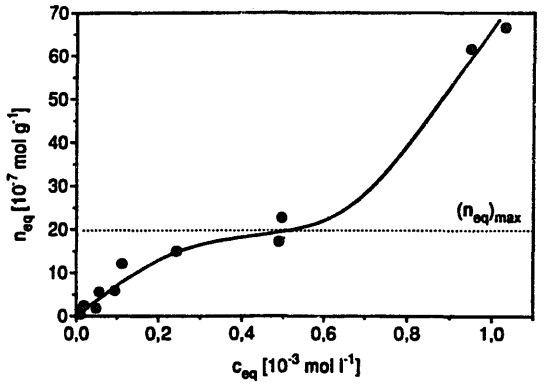

Fig. 1. Variation of the adsorbed amount of **1a** per gram of CdS (n_{eq}) in equilibrium with a methanolic solution of **1a** (c_{eq}).

has previously been applied to the adsorption of alcohols onto TiO_2 [7,8,13]. The model assumes the formation of an ideal mixed solute–solvent monolayer, as formulated by Eq. (10) and Eq. (11), in which a_1 and a_2 are the activities of methanol and **1a** in bulk solution (b) and at the surface (s) respectively

$$a_1^s + a_2^b \underset{k_{des}}{\overset{k_{ad}}{\rightleftharpoons}} a_1^b + a_2^s \tag{10}$$

$$K' = \frac{a_1^b a_2^s}{a_1^s a_2^b} \tag{11}$$

With the relations $K=K'(a_1^b)^{-1}$ and $a_2^b \approx c_{eq}$, Hiemenz [14] arrived at

$$\frac{c_{eq}}{n_{eq}} = \frac{N_A\sigma^0}{A_{sp}K} + \frac{N_A\sigma^0}{A_{sp}}c_{eq} \tag{12}$$

in which σ^0 is the average area per imine molecule in the monolayer surface phase when it is saturated by the imine, A_{sp} is the specific surface area of CdS (70 m^2 g^{-1}) and N_A is Avogadro's number. Fig. 2 shows a plot of $c_{eq}(n_{eq})^{-1}$ vs. c_{eq}, exhibiting considerable deviations from the expected linearity (0.90, least-squares regression coefficient). Repeated experiments suggest that this is due to errors in the measurement of the very low concentration changes and in obtaining identical suspensions. From the slope and intercept, a value of 4400 ± 950 l mol^{-1} is calculated for the adsorption constant K. From this, the average area of the adsorbed imine

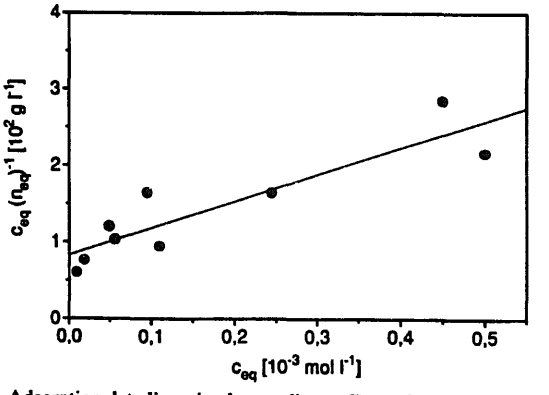

Fig. 2. Adsorption data linearized according to Eq. (12); intercept $b=82.4$ 15.6 g l^{-1}; slope $m=(3.5\pm0.6)\cdot10^5$ g mol^{-1}; correlation coefficient, 0.90.

(σ^0) is obtained from Eq. (12) as 40 nm^2. This is far too large as indicated by a comparison with the value of 0.5 nm^2 (1.40 nm×0.35 nm) estimated for a flat unsolvated molecule. This suggests that only 1%–2% of the surface is covered by **1a** in competition with the solvent. Assuming a size of 0.08 nm^2 (0.30 nm×0.25 nm) for one methanol molecule, we estimate that a 500-fold excess of the solvent is present in the surface monolayer. Although these values should be considered with care, they are not unexpected since methanol should adsorb more strongly than **1a** onto the hydrous CdS surface [16].

3.2. Dependence of the reaction rate on the concentration of 1a

In order to obtain the pseudo-adsorption constant, the imine disappearance rate was measured at different initial concentrations of **1a** by determining the slopes of the concentration vs. time curves (Fig. 3). It is noted that the two products **2a** and **3a** are formed in about equal amounts. After a short induction period, the reaction is zero order at concentrations above 0.5 mmol l^{-1} (Fig. 3(a)) but first order below (Fig. 3(b)). Thus we would expect that, for experiments 1 and 2 (Fig. 3(a)), the same rates should be obtained at a given imine concentration, e.g. at 1.0 mmol l^{-1}. Since this is not the case, we must assume that the amount of light absorbed changes with varying substrate concentration. This effect does not depend on the length of the sonication time, since similar results were obtained when this was 3 h instead

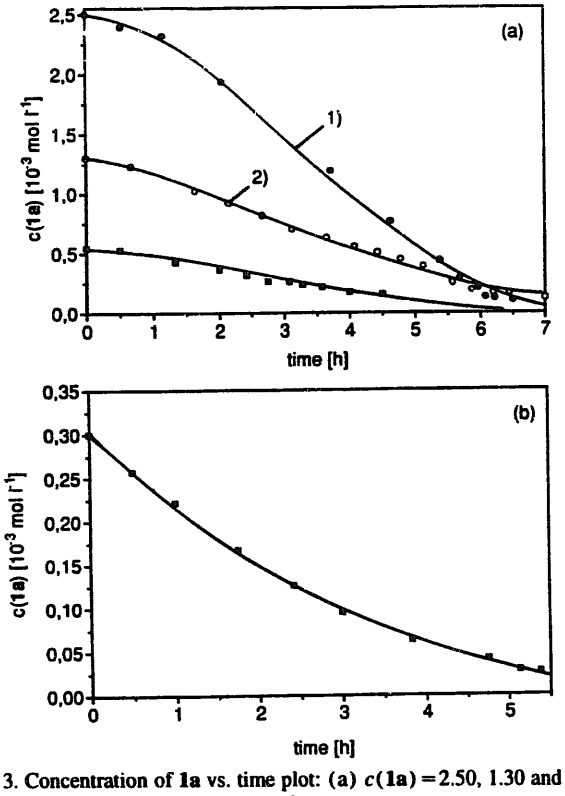

Fig. 3. Concentration of **1a** vs. time plot: (a) c(**1a**) = 2.50, 1.30 and 0.54 mmol l^{-1}; (b) c(**1a**) = 0.30 mmol l^{-1}; from a first-order decay, we obtain $k = 7.6 \times 10^{-5}$ s^{-1}.

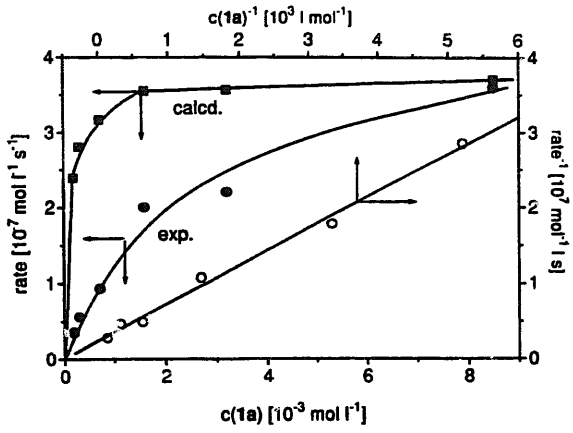

Fig. 4. Experimental and calculated reaction rate dependence on c(**1a**); double-reciprocal plot according to Eq. (13).

of the usually applied 15 min. However, the data obtained were analyzed further to allow a comparison with the more reliable "in situ" method (see below). The similar dependence of the reaction rate (see Section 2) and amount of adsorbed **1a** (Fig. 1) on the initial concentration points to the dominant role of substrate adsorption.

From a double-reciprocal plot [17,18], according to Eq. (13) ($k'_{red} = k_{red}[H^+]_{ad}[e_r^-](n_{eq})_{max}$)

$$\frac{1}{\text{rate}} = \frac{1}{k'_{red}} + \frac{1}{k'_{red}K_r}\frac{1}{c(\mathbf{1a})} \qquad (13)$$

we calculate a pseudo-adsorption constant of $K_r = 520 \pm 90$ l mol^{-1} (Fig. 4). This value is only about 12% of the true constant obtained in the dark adsorption experiments. To obtain a better comparison, the calculated rates (see Section 2) are also displayed in Fig. 4. The discrepancy probably arises from an increase in the light-absorbing surface area which would explain the superproportional rate increase at imine concentrations higher than 0.5 mmol l^{-1}. These changes in the surface properties seem to occur on preparation of the suspension prior to irradiation, since a linear concentration decrease is observed during the photoreaction. In agreement with this explanation, a strong increase of imine adsorption was found in this concentration range (Fig. 1).

In order to prevent the problems encountered in the preparation of identical CdS suspensions at different imine concentrations, the dependence of the reaction rate was measured by a type of "in situ" method in one unique experiment. The rate at a given concentration was calculated by constructing the tangent at the corresponding point of the decay curve of **1a**. In Fig. 5, the results are displayed for two initial concentrations below 0.6 mmol l^{-1}, as well as the double-reciprocal plots according to Eq. (13). The average value (see Section 2) of the "in situ" adsorption constant $K_i = 2000$ l mol^{-1} is about 70% of the true value and therefore fits much better than the value obtained from the conventional kinetic experiments.

That it still differs significantly can be understood in terms of a perturbation of the Langmuir type of adsorption equilib-

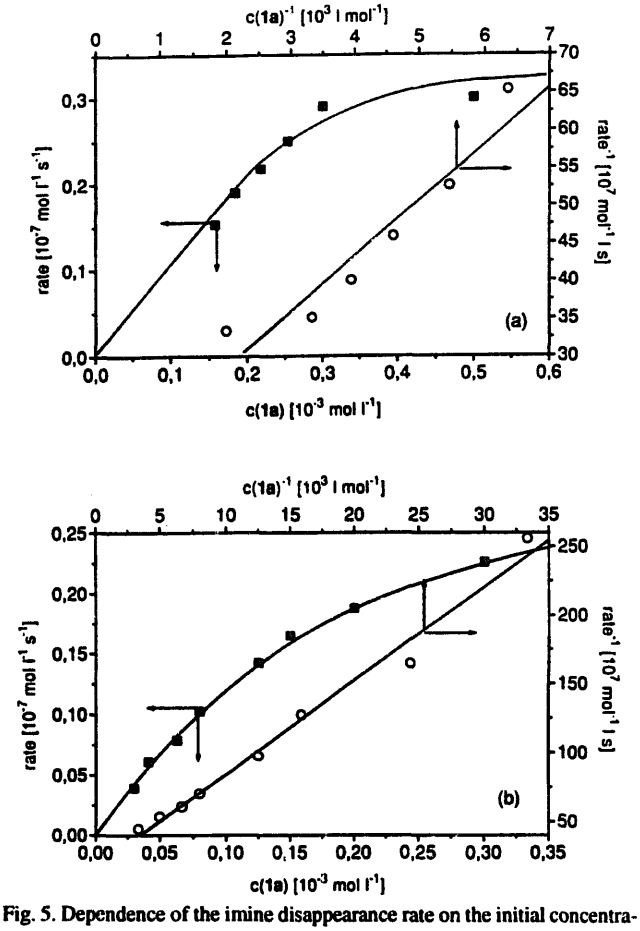

Fig. 5. Dependence of the imine disappearance rate on the initial concentrations obtained from the "in situ" method; double-reciprocal plots according to Eq. (13); initial concentrations of **1a** are 0.54 mmol l^{-1} (a) and 0.30 mmol l^{-1} (b).

rium due to substrate consumption. This can be accounted for by introducing the term $k'_{red}\theta(\mathbf{1a})$ in the expression for the change in surface coverage with time

$$\frac{d\theta(\mathbf{1a})}{dt} = k_{ad}(1-\theta)c(\mathbf{1a}) - k_{des}\theta(\mathbf{1a}) - k'_{red}\theta(\mathbf{1a}) \quad (14)$$

Assuming stationary conditions, i.e. $d\theta(\mathbf{1a})/dt = 0$, we arrive at Eq. (15) and the equilibrium constant is then given by Eq. (16). Thus kinetic measurements are expected to afford smaller values, although the difference depends on the ratio of the rate constants involved.

$$\theta(\mathbf{1a}) = \frac{k_{ad}c(\mathbf{1a})}{k'_{red} + k_{des} + k_{ad}c(\mathbf{1a})} = \frac{K_r c(\mathbf{1a})}{1 + K_r c(\mathbf{1a})} \quad (15)$$

$$K_r = \frac{k_{ad}}{k'_{red} + k_{des}} \quad (16)$$

Further complication may arise from the photoadsorption of the substrates or products as known to occur in the system TiO_2/O_2 [19].

3.3. Dependence of the reaction rate on the olefin concentration

Since in dark adsorption studies no concentration change was observable by HPLC analysis, only the pseudo-adsorption constant could be measured through application of the kinetic method. Unfortunately, the "in situ" procedure could not be employed since, at the low cyclopentene concentrations necessary to observe a first-order reaction, an olefin-independent photolysis of **1a** successfully competed with the addition reaction. In the absence of cyclopentene, the photolysis rate was 0.2×10^{-7} mol l^{-1} s^{-1}. Therefore this value was subtracted from all the measured disappearance rates of **1a**. As discussed above, the data can be analyzed in terms of Eq. (13); $c(\mathbf{1a})$ and k'_{red} must be replaced by the olefin concentration and k'_{ox} respectively, and the rate becomes equal to $k_{ox}[h_r^+]_{ss}[RH]_{ad}$ (Eq. (6)). The results for cyclopentene and cyclohexene are summarized in Fig. 6 from which the pseudo-constants of 15 and 13 l mol^{-1} respectively are obtained. Although the absolute values must be treated with care (see above), their similarity indicates that both olefins are adsorbed to the same extent as further corroborated by competition experiments.

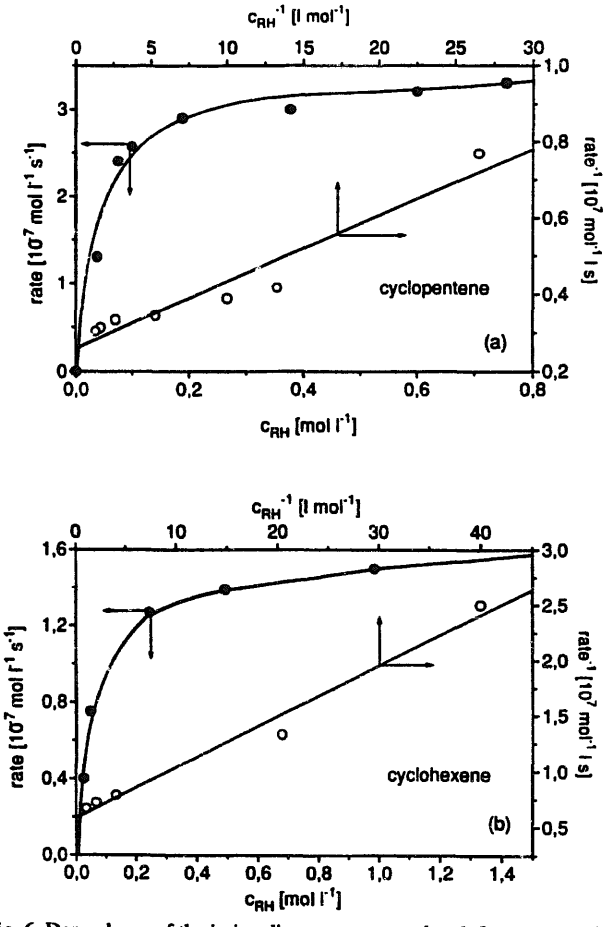

Fig. 6. Dependence of the imine disappearance on the olefin concentration; double-reciprocal plots according to Eq. (13). (a) Cyclopentene, $c(\mathbf{1a}) = 7.0$ mmol l^{-1}. (b) Cyclohexene, $c(\mathbf{1a}) = 3.0$ mmol l^{-1}.

Since, in the case of cyclohexene, the addition product has a similar retention time to the hydrodimer of **1a**, the imine **1b** was employed in the competition experiment. Cyclopentene addition to **1b** was 1.4 times faster than for cyclohexene and afforded more of the hydrodimer (**2b** : **3b** = 0.85; **4b** : **3b** = 5.0), while the imine disappearance rate was accelerated 3.3 times. When the competition experiment was performed in the presence of equal amounts of the two olefins (1.0 mmol l^{-1}, in order to be in the range of saturation coverage), the rates of both addition and hydrodimerization were decreased by 50%. As an example, the latter had a measured rate of 0.32×10^{-7} mol l^{-1} s^{-1} which matches very well half of the sum of the rates of the two independent reactions ($0.5\times0.63+0.5\times0.08=0.36\times10^{-7}$ mol l^{-1} s^{-1}). In addition to supporting the same strength of adsorption for both olefins, these results strongly suggest that they are adsorbed onto the same surface sites.

3.4. Influence of the light intensity and CdS concentration

Decreasing the light intensity to 10%–50% of its original value results in a linear decrease in the reaction rate. Above 50%, a saturation effect is observed. This is in accord with other photoreactions catalyzed by semiconductor powders [18,20,21]. At higher intensities, the rate increases usually proportionally to $I_a^{1/2}$ due to enhanced charge recombination, as reported for the TiO_2-catalyzed (specific surface area, 7 m^2 g^{-1} [20]) photo-oxidation of isopropanol at light intensities above 10^{16} quanta s^{-1}. In the system investigated here, this occurs only above 10^{18} quanta s^{-1} (see Section 2). The much larger specific surface area of CdS (70 m^2 g^{-1}) results in a lower electron–hole surface concentration and therefore in a low rate of charge recombination. Therefore a higher light intensity is required to make the latter process fast enough compared with the interfacial electron transfer from and to the adsorbed substrates. It should be noted that the product ratio **2a** : **3a** = 0.9 does not depend on the light intensity. Assuming that reductive and oxidative reaction steps (Eq. (5) and Eq. (6)) are coupled, the rates of α-aminobenzyl and cyclopentenyl radical formation should be equal. When the concentrations of these radicals are taken as equal, we arrive at rate laws for product formation which differ only by the rate constants k_{add} and k_{dim}. Therefore their ratio should also determine the ratio of **2a** : **3a**. The fact that the latter does not change suggests that these rate constants are independent of the light intensity.

As observed for the photoreduction of methyl orange [17] and the oxidative photodimerization of olefins [18] catalyzed by CdS powder, the dependence of the rate on the CdS concentration increases linearly and reaches a plateau at about 3 g l^{-1} (Table 1).

Surprisingly, in the same concentration range, the ratio of addition to hydrodimer production decreases from two to about unity. As can be seen in Table 1, the specific rate v_s (rate divided by the amount of CdS employed) decreases from 4.7×10^{-7} mol g^{-1} s^{-1} at 0.34 g l^{-1} of CdS to 0.8×10^{-7} mol g^{-1} s^{-1} at 6.70 g l^{-1} of CdS. The surface concentration of the intermediate radicals should therefore be lower at large amounts of CdS, but the ratio of the α-aminobenzyl to cyclopentenyl radical concentration will not change. Therefore the product ratio should remain constant. However, a lower concentration of radicals increases their lifetime when it is assumed that they undergo only second-order decay reactions. This effect should favor hydrodimerization which is a $2e^-/2h^+$ process and therefore requires that the second radical pair is generated during the lifetime of the first. A closer inspection of the heterocoupling and homocoupling steps (Eq. (7) and Eq. (8)) further supports this explanation when we make the plausible assumption that these reactions occur at different surface sites. Although the distance between the reactive electron–hole pair and therefore between the α-aminobenzyl and cyclopentenyl radicals is not known, it should be closer than the distance between two like radicals and the latter should increase with increasing amounts of CdS. This means that homocoupling (affording **3a**) requires a longer diffusion path than heterocoupling (affording **2a**). The increased lifetime of the radicals leads to larger diffusion lengths and therefore favors the homocoupling reaction.

Table 1
Rate dependence on the amount of CdS

Rate/ratio	CdS (g l^{-1})					
	0.34	0.67	1.07	2.0	3.34	6.7
v [a]	1.6	2.1	3.7	4.5	5.6	5.5
2a : **3a**	2.0	1.5	1.3	1.2	0.95	0.9
v_s [b]	4.7	3.1	3.5	2.3	1.7	0.8

[a] Disappearance rate of **1a** (10^{-7} mol l^{-1} s^{-1}).
[b] Obtained by dividing v by the amount of CdS (10^{-7} mol g^{-1} s^{-1}).

Acknowledgements

We are grateful to Professor Dr. G. Emig for the measurement of the surface areas, and to the Fonds der Chemischen Industrie and Volkswagen Stiftung for financial support.

References

[1] H. Gerischer, *J. Phys. Chem., 88* (1984) 6096.
[2] A.J. Bard, *Science, 207* (1980) 139. A.J. Bard, *J. Phys. Chem., 86* (1982) 172.
[3] G. Hodes, I.D.J. Howell and L.M. Peter, *J. Electrochem. Soc., 139* (1992) 3136. A. Wahl, M. Uhlmann, A. Carroy and J. Augustynski, *J. Chem. Soc., Chem. Commun.*, (1994) 2277. B. Ohtani and S. Nishimoto, *J. Phys. Chem., 97* (1993) 920.
[4] N. Serpone, D.K. Sharma, M.A. Jamieson and M. Grätzel, *Chem. Phys. Lett., 115* (1985) 473. R. Rossetti and L.E. Brus, *J. Phys. Chem., 90* (1986) 558. J.P. Kuczynski, B.H. Milosavijevic and J.K. Thomas, *J. Phys. Chem., 87* (1983) 3368.
[5] H. Kisch, *J. Prakt. Chem., 336* (1994) 635.

[6] M.A. Fox and M.T. Dulay, *Chem. Rev., 93* (1993) 635.
[7] J. Cunningham and S. Srijaranai, *J. Photochem. Photobiol. A: Chem., 58* (1991) 361.
[8] J. Cunningham and P. Sedlák, *J. Photochem. Photobiol. A: Chem., 77* (1994) 255.
[9] C. Amatore and A.R. Brown, *J. Am. Chem. Soc., 118* (1996) 1482.
[10] R. Künneth, Ch. Feldmer and H. Kisch, *Angew. Chem., 104* (1992) 1102. R. Künneth, Ch. Feldmer, F. Knoch and H. Kisch, *Chem. Eur. J., 1* (1995) 441.
[11] W. Schindler, F. Knoch and H. Kisch, *Chem. Ber., 129* (1996) 925.
[12] Y. Nosaka, Y. Ishizuka and H. Miyama, *Ber. Bunsenges. Phys. Chem., 90* (1986) 1199, and references cited therein.
[13] J. Cunningham and G. Al-Sayyed, *J. Chem. Soc., Faraday Trans., 86* (1990) 3935.
[14] P.C. Hiemenz, *Principles of Colloidal and Surface Chemistry*, M. Dekker, New York, 2nd edn., 1986.
[15] R.S. Hansen and R.P. Craig, *J. Phys. Chem., 58* (1954) 211.
[16] S.W. Park and C.P. Huang, *J. Colloid Interface Sci., 128* (1989) 245.
[17] A. Mills and G. Williams, *J. Chem. Soc., Faraday Trans. 1, 83* (1987) 2647.
[18] H. Al-Ekabi and P. de Mayo, *Tetrahedron, 42* (1986) 6277.
[19] W.G. Becker and A.J. Bard, *J. Phys. Chem., 87* (1983) 4888.
[20] T.A. Egerton and C.J. King, *J. Oil. Col. Chem. Assoc., 62* (1979) 386.
[21] L. Vincze and T.J. Kemp, *J. Photochem. Photobiol. A: Chem., 87* (1995) 257.